LA-UR- 09-01026

Approved for public release;
distribution is unlimited.

Title:	Nitrogen isotopes in the recent solar wind from the analysis of Genesis targets: evidence for large scale isotopic heterogeneity in the nascent Solar System
Author(s):	Bernard Marty, Laurent Zimmermann, Peter G. Burnard, Donald S. Burnett, Roger C. Wiens, Veronika S. Heber, Rainer Wieler, and Peter Bochsler
Intended for:	Science

Los Alamos
NATIONAL LABORATORY
EST. 1943

Form 836 (7/06)

Nitrogen isotopes in the recent solar wind from the analysis of Genesis targets : evidence for large scale isotope heterogeneity in the nascent Solar System

Bernard Marty[1], Laurent Zimmermann[1], Peter G. Burnard[1], Donald L. Burnett[2], Roger C. Wiens[3], Veronika S. Heber[4], Rainer Wieler[4], & Peter Bochsler[5]

[1]Centre de Recherches Pétrographiques et Géochimiques, Nancy Université, INSU-CNRS, BP20, 54501 Vandoeuvre lès Nancy Cedex, France. bmarty@crpg.cnrs-nancy.fr
[2]Department of Geological and Planetary Sciences, Caltech, Pasadena, CA 91125, USA.
[3]Los Alamos National Laboratory, Los Alamos, NM 87545, USA.
[4]Isotope Geology and Mineral Resources, ETH Zürich NW, Clausiusstrasse 25, CH-8092, Switzerland.
[5]Physicalisches Institut, University of Bern, Sidlerstrasse 5, CH-3012 Bern, Switzerland.

Nitrogen, the fifth most abundant element in the universe, displays the largest stable isotope variations in the solar system reservoirs after hydrogen. Yet the value of isotopic composition of solar nitrogen, presumably the best proxy of the protosolar nebula composition, is not known. Nitrogen isotopes trapped in Genesis spacecraft target material indicate a 40 % depletion of ^{15}N in solar wind N relative to inner planets and meteorites, and define a composition for the present-day Sun undistinguishable from that of Jupiter's atmosphere. These results indicate that the isotopic composition of of nitrogen in the outer convective zone of the Sun (OCZ) has not changed through time, and is representative of the protosolar nebula. Large ^{15}N enrichments during e.g., irradiation, or contributions from ^{15}N-rich presolar components, are required to account for planetary values.

The causes of N isotope variations among solar systems reservoirs (Fig. 1) are essentially discussed in terms of mixing between different solar, possibly presolar, reservoirs (e.g., (1)) isotopically fractionated to different extents. Knowledge of the N isotopic composition of the Sun, which is by far the largest reservoir of N in the solar system, and presumably reflects protosolar nebula composition quite closely, will shed light on the bulk composition of the protosolar nebula, giving a framework to locate sources of different components in the solar system, to establish a taxonomy of planetary materials, and to investigate processes responsible for isotopic fractionation of light elements in the nascent solar system. Spectroscopic methods have not determined the N isotopic composition of the Sun with the required accuracy. Most attempts of determination have been indirect, based either on the

analysis of the atmospheres of giant planets or of the solar wind (SW) trapped in lunar soils. The latter led to the concept of an allegedly secular variation of the SW $^{15}N/^{14}N$ ratio (2). Soils presumably exposed long (1-3 Ga) ago tend to be poor in ^{15}N by at least 20 % relative to "planetary" N (here the term planetary is referring essentially to inner solar system bodies : Earth, Mars interior, Venus and most primitive meteorites; all these objects have bulk N isotope ratios within 5 % of the terrestrial value, $^{15}N/^{14}N = 3.676 \times 10^{-3}$ for the terrestrial atmosphere), whereas soils exposed more recently during the last ~200 Ma show ^{15}N enrichments (e.g., (3, 4)). Any explanation of a secular variation of the solar source faces serious astrophysical problems (see ref. (1)), so that mixing between non-solar and solar N components at the Moon's surface (e.g., meteorites, interplanetary dust particles, cometary matter, terrestrial atmosphere) have been advocated instead (1, 5-8). Recently, several independent studies led their authors to conclude that nitrogen in the protosolar nebula was drastically depleted in ^{15}N compared to the terrestrial standard. These are : (i) the simultaneous ion probe analysis of H and N isotopes in lunar soil grain skins that led (8) to conclude that that SW N is depleted by more than 24 % in ^{15}N ($^{15}N/^{14}N \leq 2.8 \times 10^{-3}$); (ii) the analysis of the Jupiter atmosphere by infra-red spectroscopy (9, 10) as well as by *in-situ* mass spectrometry by the Galileo probe ($^{15}N/^{14}N = [2.3\pm0.3] \times 10^{-3}$) (11); (iii) a $^{15}N/^{14}N$ ratio of $[2.36\pm0.04] \times 10^{-3}$ for osbornite (TiN) embedded in a calcium-aluminium inclusion (CAI) of a primitive meteorite (12), regarded as being the first solid N-bearing phase to form in the cooling protosolar cloud. We believe that the solar wind provides the most authentic samples of the solar isotopic composition, and hence, of the protosolar nebula for elements heavier than boron. Here we report the results of the N isotope analysis of Genesis targets exposed to SW irradiation in space.

The Genesis spacecraft sampled SW ions during 27 months at the Lagrange point L1, by implantation of SW ions in several target materials (13). Despite a hard landing of the sample return capsule on Earth, target material was recovered and yielded information of exceptional quality on the noble gas composition of the SW (14, 15). The expected fluence of implanted SW nitrogen ions during the exposure period of 27 months is very low (1.3×10^{-12} mol $^{14}N/cm^2$, see Supplementary Online Material -SOM) in comparison to the terrestrial background in the target material and in analytical facilities (N analytical blanks are generally of the order of 10^{-10}-10^{-11} mol), requiring the development of specific cleaning and analytical procedures. Nitrogen and noble gases were extracted from the target material by laser ablation and analysed by static mass spectrometry at CRPG Nancy, France, using a new dedicated

facility (16). Gold targets were selected for this study because it allows a high extraction efficiency of nitrogen ions implanted at SW energies, a point that was checked using test targets implanted with known ^{15}N fluence and energy (16). Targets were mounted under high vacuum on a moving stage and ablated with a UV (193 nm) laser having a spot size of approx. 50x150 μm. The N procedural blanks were improved over 3 years until they reached a level of $< 2 \times 10^{-12}$ mol ^{14}N, low enough to make a few percent of N released from the targets (it turned out that atmospheric N contained in the targets was always larger than expected pure SW N, see next paragraph). Ablation was carried on with and without O_2 in the vacuum chamber to check for any chemical reactions of SW N with H and C, and no difference in the data was detected between these two types of runs (Table 1). Evolved gases were separated into two fractions and purified specifically for noble gases and nitrogen in two different line sections. By modulating the power of the laser beam or the number of pulses per unit area, it was possible to remove sequentially layers of gold with a depth resolution of a few nm. Noble gas (e.g., neon, occasionally helium and argon) abundances and isotopic ratios, analysed together with N in each extraction step, were dominated by their SW component and were used as tracers of SW occurrence, of terrestrial contamination, and of elemental and isotopic fractionations.

Despite extensive cleaning (see SOM), all target materials we analysed were found to be contaminated with terrestrial N, as evident by their N/Ne ratios which were much higher than those expected for the SW (Table 1). Correlation between extracted N and SW Ne during stepwise laser extraction demonstrated that contaminant N was present not only at the very surface (as a result of adsorption, organic contamination, or particle contribution due to the hard landing) but part was also more deeply within the gold layer where SW ions are implanted, probably introduced during target manufacturing. In an attempt to get an enhanced SW signal to noise ratio, we analyzed the so-called gold cross from the Genesis concentrator target (Fig. 2). The concentrator was an ion-focusing device designed to enhance the solar wind ion flux by an average factor of 25 (17) (Fig. 2). The gold cross was a gold-plated stainless steel frame that held four target quadrangles in the center of the concentrator. Nitrogen and noble gases were extracted by laser ablation of two radial gold cross arms (GCAs) (GCA1, JSC sample #60009.1, analysed in April-July 2007, and GCA2, JSC #60009.2, analysed in May-July 2008). Several areas of 2-6 mm^2 were ablated from the border to the centre of both GCAs (Fig. 2).

The concentrator fractionates solar wind (ref X), as observed by Ne isotopes (18), and care has to be taken for interpreting N isotope variations along the GCAs (Fig. 3). The least fractionated Ne isotopic composition similar to that of Genesis SW (14, 15) was found ~20 mm from the edge of the GCA, and depletion of the light isotope (^{20}Ne) relative to the heavy one (^{22}Ne) increased progressively along the GCA towards the center of the concentrator target (18). Both Ne contents and isotopic ratios measured in this study are comparable to those determined by (18), despite large differences in the ablated surfaces (100 μm diameter spots versus few mm^2, respectively) (see Fig. S1 in SOM). The helium isotopic ratios follow comparable isotope fractionation (see Figs. S2 and S3 in SOM). Neon 3-isotope fractionation (Fig. S2, SOM) suggests a mass-dependent law, where isotopic fractionation is proportional to $(m)^{-1/2}$. Isotopic fractionation in the concentrator also depends on the mass/charge (m/q) ratio. Nitrogen in the solar wind occurs mostly as N^{5+} with little contribution of N^{6+} ions, so that the mean N charge state is close to +5.5, and the m/q ratios of ^{14}N and ^{15}N are 2.54 and 2.73, respectively. SW neon occurs mostly as Ne^{8+}, and the m/q ratios of ^{20}Ne and ^{22}Ne are 2.50 and 2.75, respectively, very similar to those of N isotopes, yielding comparable isotopic effects. Hence isotope fractionation of implanted SW ^{15}N/^{14}N should be similar to that of ^{22}Ne/^{20}Ne, that is, a maximum of ~60 ‰ (18). Most of analysed N is from terrestrial contamination (see next paragraph), so that N isotope fractionation should have affected only the SW N component, since the concentrator was not able to process contaminant N degassed from the spacecraft, for obvious charge/energy reasons. Because SW N comprises less than 4 % of total N (Fig. 4), the overall correction for isotopic fractionation on the measured N isotope ratios is $\leq$ 3 ‰, that is, within analytical uncertainties. Notably, isotope fractionation depleted the light isotope relative to the heavy one towards the center of the concentrator target, contrary to the isotopic variations observed for N (Fig. 3). On the other hand, SW ions are more strongly concentrated towards the center of the target, where the lighter isotopic ratios are found. Thus the ^{15}N/^{14}N variations between different analyses of the GCA cannot result from concentrator fractionation, but rather indicate mixing of variable proportions of the terrestrial N contaminant and a nitrogen component depleted in ^{15}N.

We use a mixing diagram to identify the composition of the ^{15}N-poor component (Fig. 4), in which the N isotopic ratios (expressed as δ^{15}N; see Fig. 4 caption for definition) are plotted against the ^{20}Ne/^{14}N ratios normalised to the SW value. For the case of a two end-member mixing, data points define a straight line linking the two end-member compositions, and the

respective $\delta^{15}N$ values of the end-members can be determined by extrapolating the x-values ($^{20}Ne/^{14}N$) either to 0 (reflecting terrestrial N in the GCA gold layer) or to 1 (SW N). For the SW $^{20}Ne/^{14}N$ ratio, we adopt the coronal abundances derived from solar energetic particle data by (19) (see also (20)). This yields a best estimate for the SW $^{20}Ne/^{14}N$ ratio of 1.14 ± 0.23 (SOM). Within uncertainty, this value is in agreement with in-situ SW analyses: a ratio of 1.24±0.30 has been obtained recently from the ACE mission (D. B. Reisenfeld, pers. comm.). The mixing deconvolution requires also the SW Ne/N ratio to be near-constant along the GCAs. The $^{20}Ne/^{36}Ar$ ratios, which were analysed in sample GCA1 #60009.1, vary from 44.7 at the GCA edge to 38.8 close to the GCA center. These values are within a few % of the proposed unfractionated SW $^{20}Ne/^{36}Ar$ ratio of 44±2 for Genesis SW (21), suggesting that fractionation of the SW $^{20}Ne/^{14}N$ ratio due to concentrator target fractionation was of the same order and within our stated uncertainty (20 %) for this ratio.

Despite extensive nitrogen contamination of our gold target (≥ 96 % of total N is terrestrial according to our two component deconvolution), the data permit the identification of the isotopic composition the ^{15}N-poor nitrogen end-member (Fig. 4). Extrapolation to x = 0 yields $\delta^{15}N$ = 12.7±3.5 ‰ for the terrestrial end-member, consistent with $\delta^{15}N$ values measured for blank (not flown) GCAs (see SOM). The SW end-member $\delta^{15}N$ is -388±183 ‰, or $^{15}N/^{14}N$ = [2.26±0.67] x 10^{-3} (both at 2 σ level).

SW nitrogen is presumably fractionated by inefficient Coulomb drag which operates in the solar wind acceleration against solar gravity. We expect the strongest fractionation effect in low speed solar wind. In the relevant region where nitrogen decouples from the Coulomb drag exerted by protons, nitrogen appears mostly as N^{5+} or in higher charge states (see above). Compared to the observed fractionation of the neon isotopes, an effect of about 5% or less is expected between SW N in our bulk sample and nitrogen in the solar convective zone (e.g., (20)). Thus we infer, together with arguments raised before, that our SW value is representative of the N isotope ratio in the outer convective zone. As solar gravitational settling is expected to fractionate nitrogen by < 1% (ref Y), solar convective zone N is likely to represent the protosolar N isotope ratio. From the absence of an excess of ^{3}He in the outer convective zone of the Sun compared to the protosolar value (including converted deuterium) we conclude that the Sun never underwent deep mixing after the ignition of the proton-proton

cycle, and, consequently, it also did not modify the isotopic composition of N in the outer convective zone (e.g., (1)).

Our estimate for the solar N isotopic composition of [2.26±0.67] x 10^{-3} is significantly different, at the 95 % confidence level, from the terrestrial ratio of 3.676 x 10^{-3}, as well as from values measured in inner planets, in meteorites, and in comets (Fig. 1). It is, however, consistent with estimates of the protosolar nebula value ([2.3±0.3] x 10^{-3} from the Jupiter atmosphere analysis (10, 11) and [2.36±0.04] x 10^{-3} from TiN in CAI analysis (12)), re-enforcing the previous conclusion that the solar nuclear activity has not significantly affected the isotopic composition of the protosolar gas in the photosphere for elements heavier than boron.

The similarity between Jupiter and the present-day SW-N isotopic composition has implication for understanding the diversity of N isotopic ratios among solar system reservoirs (Fig. 1). The Sun indeed becomes the solar system reference for N isotopes, so that all solar system objects other than giant planets are isotopically anomalous with respect to the Sun, and must have incorporated either (i) isotopically processed solar system components, or (ii) material distinct from the one that formed the solar nebula and that never mixed with it. The facts that comets are among the most ^{15}N rich bodies analysed so far (22) (Fig. 1) and that the analysis of Stardust material supports a solar system origin for cometary matter (23) suggest a solar system origin for N isotope anomalies, as also recently proposed for large D/H anomalies in primitives meteorites (24). Based on mass balance considerations, such dramatic ^{15}N enrichments must have occurred as contributions of N-bearing solid compounds rather than under a gaseous state. The observation that HCN and CN in comets are the carriers of the ~120 % ^{15}N enrichments (22) makes a clear case that ^{15}N-rich atomic N has been involved in chemical exchange, since the major form of nitrogen in the nascent solar system was probably molecular N_2. Ion-molecule reactions are apparently unable to produce the required $\geq$ 100 % ^{15}N enrichment (25). Photodissociation of N_2 by solar EUV, with (26) or without (27) self-shielding, that would create fractionate N^+ ions to react with either H, C, and/or exchange with N compounds in the irradiated solar nebula might be responsible for this remarkable isotope heterogeneity in the nascent solar system.

We are grateful to J.H. Allton, A J.G. Jurewicz and the Genesis Curation team at Johnson Space Center, NASA, Houston (USA) for excellent sample selection and preparation. F.

Gaboriau, LCPME, Vandoeuvre Lès Nancy (France) performed atomic force microscopy analysis of test samples. S. Sestak and I.A. Franchi did ozone cleaning of the samples at the Open University, Milton Keynes (UK). We thank the members of the Genesis Science Team, in particular R.O. Pepin, for constructive intereactions during the last 6 years. We also thank the LANL concentrator instrument team for enabling this work. This study was funded by Centre National d'Etudes Spatiales, by Centre National de la Recherche Scientifique - Institut National des Sciences de l'Univers, by Région Lorraine, by Swiss National Science Foundation, and by NASA through the Genesis mission.

References

1. J. Geiss, P. Bochsler, *Geochim. Cosmochim. Acta* **46**, 529 (1982).
2. J. F. Kerridge, *Science* **188**, 162 (1975).
3. J. F. Kerridge, *Rev. Geophys.* **31**, 423 (1993).
4. J. S. Kim, Y. Kim, K. Marti, J. F. Kerridge, *Nature* **375**, 383-385 (1995).
5. R. Wieler, F. Humbert, B. Marty, *Earth Planet. Sci. Lett.* **167**, 47 (1999).
6. P. Bochsler, *Adv. Space Res.* **14/6**, 161 (1994).
7. M. Ozima *et al.*, *Nature* **436**, 655 (2005).
8. K. Hashizume, M. Chaussidon, B. Marty, F. Robert, *Science* **290**, 1142 (2000).
9. T. Fouchet *et al.*, *Icarus* **143**, 223 (2000).
10. M. M. Abbas *et al.*, *Ap. J.* **602**, 1063 (2004).
11. T. Owen, P. R. Mahaffy, H. B. Niemann, S. Atreya, M. Wong, *Ap. J.* **553**, L77 (2001).
12. A. Meibom *et al.*, *Ap. J.* **656**, L33 (2007).
13. D. S. Burnett *et al.*, *Space Sci. Rev.* **105**, 509 (2003).
14. A. Grimberg *et al.*, *Science* **314**, 1133 (2006).
15. A. Meshik *et al.*, *Science* **318**, 433 (2007).
16. L. Zimmermann, B. Marty, P. G. Burnard, F. Gaboriaud, *Geostand. Geoanal. Res.* Submitted (2009).
17. J. E. Nordholt *et al.*, *Space Sci. Rev.* **105**, 561 (2003).
18. V. S. Heber *et al.*, *Space Sci. Rev.* **130**, 309 (2007).
19. D. V. Reames, *Adv. Space Res.* **15**, 41-51 (1995).
20. P. Bochsler, *Astron. Astrophys. Rev.* **14**, 1-40 (2007).
21. A. Grimberg et al., *Geochim.Cosmochim.Acta* **72**, 626 (2008).
22. D. Bockelee-Morvan *et al.*, *Ap. J.* **679**, L49 (2008).
23. D. Brownlee *et al.*, *Science* **314**, 1711 (2006).
24. L. Remusat *et al., Earth Planet. Sci. Lett.* **243**, 15 (2006).
25. E. Herbst, *Space Sci. Rev.* **106**, 293-304 (2003).
26. R. N. Clayton, *Nature* **415**, 860-861 (2002).
27. S. Chakraborty, M. Ahmed, T. L. Jackson, M. H. Thiemens, *Science* **321**, 1328-1331 (2008).
28. H. B. Niemann *et al.*, *Nature* **438**, 779-784 (2005).

Ref. X. R.C. Wiens *et al.*, *Space Sci. Rev.* **105**, 601 (2003).

Ref. Y. P. Bochsler, *Rev. Geophys.* **38**, 247 (2000).

	Ablated surface mm^2	^{20}Ne 10^{-14} mol/mm^2	2 σ	$^{20}Ne/^{22}Ne$	2 σ	^{14}N 10^{-12} mol/mm^2	2 σ	$\delta^{15}N$ ‰	2 σ	$\delta^{15}N$ corr MF ‰	$(^{20}Ne/^{14}N)_{sw}$ 10^{-2}	2 σ
GCA1 #6009.1												
Area1-1	**4.00**											
C43		0.14	0.003	14.00	0.71	0.51	0.19	5.8	68	5.8	0.25	0.05
C44		4.05	0.09	14.15	0.35	5.58	0.19	8.3	7.7	8.3	0.64	0.13
TOTAL		**4.19**	**0.09**	**14.14**	**0.34**	**6.09**	**0.37**	**8.1**	**9.1**	**8.1**	**0.60**	**0.12**
Area1-2	**4.84**											
C45		0.31	0.01	13.81	0.85	0.40	0.15	5.0	71	4.9	0.69	0.14
C46		9.72	0.19	13.81	0.34	9.54	0.16	12.0	5.8	11.9	0.89	0.18
C47		1.45	0.03	14.09	0.46	2.08	0.15	9.1	13.6	9.1	0.61	0.12
C48		0.51	0.01	13.58	0.47	0.63	0.15	6.4	45.4	6.3	0.71	0.14
TOTAL		**12.0**	**0.2**	**13.84**	**0.28**	**12.6**	**0.6**	**11.0**	**5.9**	**11.0**	**0.83**	**0.17**
Area1-3	**4.84**											
C50		**17.3**	**0.2**	**13.75**	**0.34**	**11.92**	**0.15**	**4.4**	**5.5**	**4.3**	**1.28**	**0.26**
Area1-4	**4.84**											
C51		0.64	0.02	13.08	0.36	0.19	0.15	-	-	-	2.95	0.59
C52		14.7	0.3	13.25	0.35	6.68	0.15	4.4	6.4	3.6	1.93	0.39
C53		9.83	0.25	13.19	0.49	5.21	0.15	4.3	7.2	3.6	1.66	0.33
TOTAL		**25.2**	**0.6**	**13.22**	**0.28**	**12.1**	**0.5**	**4.4**	**5.4**	**4.1**	**1.83**	**0.37**
Area1-5	**6.26**											
C54		6.72	0.16	13.49	0.48	1.78	0.12	0.5	13.7	-0.3	3.32	0.66
C55		39.0	1.0	13.35	0.41	9.54	0.12	7.4	6.2	6.2	3.59	0.72
TOTAL		**45.7**	**1.1**	**13.37**	**0.36**	**11.3**	**0.2**	**6.3**	**5.6**	**5.2**	**3.54**	**0.71**
Area1-6	**1.62**											
C57		**15.0**	**0.3**	**13.11**	**0.32**	**4.95**	**0.46**	**4.4**	**17.8**	**3.1**	**2.66**	**0.53**
GCA2 #6009.2												
Area 2-1-1	**4.06**											
C82		0.12	0.01	12.92	0.88	0.12	0.13	-	-	-	0.88	0.18
C83		2.92	0.22	14.44	0.57	3.56	0.13	11.3	11.2	11.5	0.72	0.14
C84		2.25	0.17	13.81	0.48	3.53	0.13	10.7	13.3	10.6	0.56	0.11
TOTAL		**5.29**	**0.40**	**14.13**	**0.38**	**7.20**	**0.39**	**11.0**	**8.6**	**11.1**	**0.64**	**0.13**
Area 2-1-2	**4.06**											
C85	4.06	0.14	0.01	12.83	0.66	0.21	0.13	-	-	-	0.60	0.13
C86	4.06	2.06	0.15	13.68	0.45	3.10	0.13	22.8	10.3	22.7	0.58	0.12
C87	4.06	3.26	0.24	13.76	0.43	5.86	0.13	3.5	8.4	3.4	0.49	0.10
TOTAL	**4.06**	**5.46**	**0.41**	**13.70**	**0.31**	**9.17**	**0.26**	**10.2**	**6.5**	**10.1**	**0.52**	**0.10**
Area 2-2	**7.19**											
C98		5.77	0.45	13.95	0.42	4.80	0.07	8.1	6.9	8.1	1.05	0.21
C99		3.49	0.27	13.71	0.41	3.67	0.07	7.7	7.6	7.6	0.84	0.17
TOTAL		**9.26**	**0.72**	**13.86**	**0.30**	**8.46**	**0.15**	**7.9**	**5.1**	**7.9**	**0.96**	**0.19**
Area 2-3-1	**4.06**											
C88		0.20	0.02	13.14	0.65	0.09	0.13	-	-	-	1.87	0.37
C89		15.1	1.1	13.75	0.40	7.12	0.13	13.1	7.8	12.9	1.86	0.37
TOTAL		**15.3**	**1.1**	**13.74**	**0.40**	**7.21**	**0.26**	**13.1**	**7.8**	**12.9**	**1.86**	**0.37**
Area 2-3-2	***4.06***											
C90		***16.3***	***1.2***	***13.54***	***0.42***	***8.44***	***0.13***	***9.1***	***6.9***	***8.7***	***1.69***	***0.34***
Area 2-4-1	**4.06**											
C91		20.7	1.5	13.56	0.41	7.89	0.13	-0.6	7.6	-1.1	2.30	0.46
C102		8.76	0.66	13.27	0.41	3.74	0.13	12.8	10.8	12.1	2.05	0.41
TOTAL		**29.4**	**2.2**	**13.48**	**0.31**	**11.6**	**0.3**	**3.7**	**6.2**	**3.1**	**2.22**	**0.44**
Area 2-4-2	***3.44***											
C96		*17.9*	*1.3*	*13.47*	*0.41*	*9.83*	*0.15*	*6.5*	*7.0*	*6.1*	*1.60*	*0.32*
C97		*6.82*	*0.52*	*12.98*	*0.41*	*4.51*	*0.15*	*8.0*	*9.2*	*7.3*	*1.33*	*0.27*
TOTAL		***24.8***	***1.9***	***13.33***	***0.32***	***14.3***	***0.3***	***7.0***	***5.6***	***6.5***	***1.51***	***0.30***
Area 2-5-1	**3.45**											
C92		25.5	1.9	13.35	0.40	7.80	0.15	-0.9	7.3	-1.9	2.87	0.57

C94		8.93	0.67	13.23	0.41	3.46	0.15	0.2	12.9	-0.7	2.26	0.45
TOTAL		**34.4**	**2.6**	**13.32**	**0.32**	**11.3**	**0.3**	**-0.6**	**6.4**	**-1.5**	**2.68**	**0.54**
Area 2-5-2	***2.63***											
C93		*26.9*	*2.0*	*13.33*	*0.41*	*9.80*	*0.20*	*0.7*	*8.6*	*-0.1*	*2.41*	*0.48*
C95		*13.8*	*1.0*	*13.21*	*0.41*	*5.18*	*0.20*	*5.3*	*9.3*	*4.3*	*2.35*	*0.47*
TOTAL		***40.8***	***3.0***	***13.29***	***0.30***	***15.0***	***0.4***	***2.3***	***6.5***	***1.4***	***2.39***	***0.48***
Area 2-6	**2.34**											
C100		25.4	1.9	13.30	0.40	6.37	0.23	-6.6	8.4	-7.9	3.50	0.70
C101		7.22	0.54	13.23	0.44	1.92	0.23	0.9	27.3	-0.4	3.29	0.66
TOTAL		**32.7**	**2.4**	**13.28**	**0.33**	**8.30**	**0.45**	**-4.9**	**9.0**	**-6.1**	**3.45**	**0.69**

Table 1 : Nitrogen and neon data for gold cross arms GCA1 (JSC# 60009.1) and GCA2 (JSC # 60009.2). Area numbers (1st column) refer to the analysed GCA (1st digit), the area location starting from the edge of the GCA (2nd digit) (see Fig. 2 for GCA2), and, when two subareas from the same location were ablated, the subarea number (3rd digit). Areas were rastered either once, with 50 laser pulses for each spot, or sequentially by increasing the number of pulses. "$\delta^{15}N$ corr MF" refers to measured $\delta^{15}N$ values corrected for concentrator target isotope fractionation, assuming mass dependency for nitrogen isotopes as inferred from He and Ne isotope data (see SOM), and using isotope fractionation observed for conjointly measured $^{20}Ne/^{22}Ne$ ratios. Only the SW N fractions, estimated from $^{20}Ne/^{14}N$ ratios, are corrected. Note that this correction is small compared to observed $\delta^{15}N$ variations. All extractions were run in vacuum, except those given in italics for which an oxygen partial pressure of ~20 Pa was present.

Figures

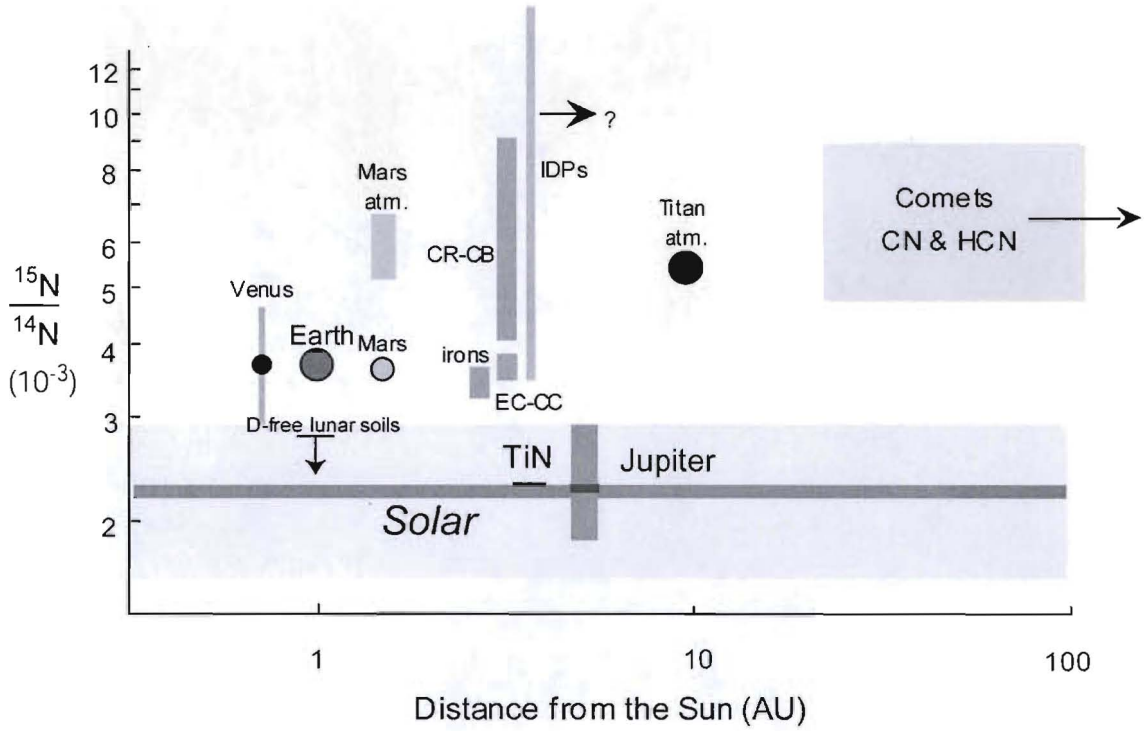

Fig.1: Nitrogen isotope variations in solar system reservoirs as a function of the distance from the Sun. Excluding the Mars atmosphere the composition of which is the result of secondary processing, and possibly the Titan atmosphere for the same reason, there seems to exist a radial evolution of the $^{15}N/^{14}N$ ratio. Jupiter's atmosphere makes an exception, because this planet presumably accreted N_2 from the protosolar nebula. Possible mass exchanges between reservoirs are illustrated by some of the meteorite and interplanetary dust particle (IDP) values, suggesting that enrichment process(es) took place in the outer solar system. Data from (3, 8-12, 22, 28) and refs. therein. The solar composition is from this work.

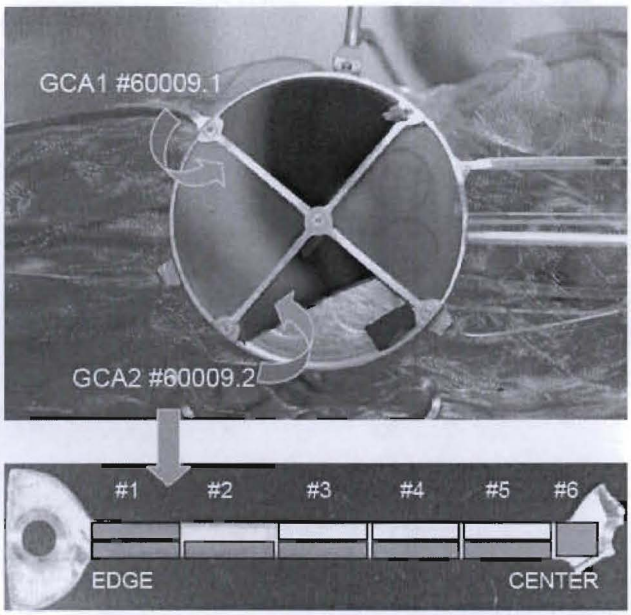

Fig. 2: The concentrator targets after recovery (top, diameter : 62 mm). The circular frame is made of stainless steel covered with Au, a material suitable for our analytical protocol. Two gold cross arms (GCAs) were analysed. For each arm, several areas were rastered with a UV laser. The areas are labelled at the bottom for GCA2, #60009.1. Numbers refer to area data given in Table 1. Ginger colour : extraction performed under high vacuum. White surface : extraction done with an oxygen pressure of ~20 Pa in the sample chamber during laser ablation. The latter was applied to check if nitrogen could have reacted to produce compounds with solar wind H and C instead of yielding N_2, which was the analysed molecule. Results (Table 1) show no difference in the data between the two methods. Photo credits : NASA (top), CRPG Nancy (bottom).

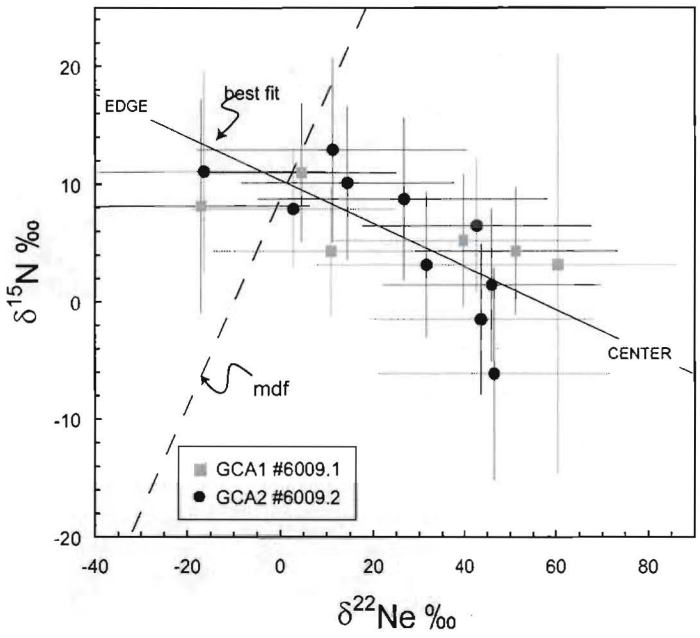

Fig. 3: Nitrogen isotopic ratios (expressed as $\delta^{15}N = [(^{15}N/^{14}N)_{sample}/(^{15}N/^{14}N)_{ATM} -1] \times 1000$, where ATM stands for atmospheric nitrogen) versus neon isotopic ratios (expressed as $\delta^{22}Ne = [(^{22}Ne/^{20}Ne)_{sample}/(^{22}Ne/^{20}Ne)_{SW} -1] \times 1000$, where SW stands for the average solar wind composition measured in Genesis material (15, 21)). Error bars are 2 σ. The solid line is the error-weighted best fit. The dotted curve represents evolution of isotopic ratios upon mass-dependent fractionation, assuming proportionality to $(m)^{-1/2}$, since Ne isotopic variations are consistent with such dependency (see SOM). The anchor values are $\delta^{22}Ne = 0$ (SW) for neon, and $\delta^{15}N = 10$ ‰, the intersection between $\delta^{22}Ne = 0$ and the best fit line. The latter is within the analytical range for the analysis of a GCA spare sample (that is, a duplicate gold cross that did not fly). Whatever the choice of mass dependency and of starting values, mass-dependent fractionation will enrich light isotopes with respect to heavy ones. Nitrogen isotopic evolution from the edge of the GCAs to their centers does not follow such a mass-dependent fractionation, and rather calls for mixing between contaminant N and another nitrogen component poor in ^{15}N.

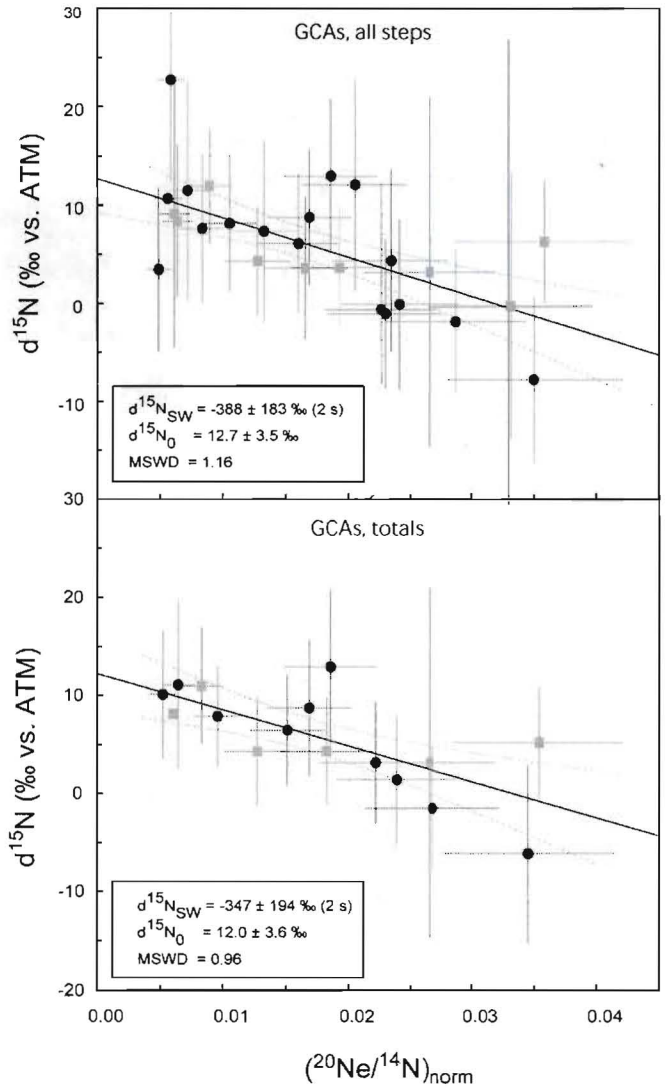

Fig. 4 : The nitrogen isotopic ratios versus the $^{20}Ne/^{14}N$ ratios normalised to the SW $^{20}Ne/^{14}N$ ratio of 1.14 ± 0.23 (see text and SOM). Error bars are 2 σ. $\delta^{15}N$ data have been corrected for mass-dependent isotopic fractionation using the conjointly measured Ne isotopic ratios. Only the fraction of SW N as estimated from the $(^{20}Ne/^{14}N)_{norm}$ ratio has been corrected. The correction varies between 0 ‰ and 1.9 ‰ at maximum, and thus has no discernable effect on the correlation. Top panel : all step ablation data, bottom panel, total (sum of all steps for a given area) data. Due to the larger number of data, the former gives a slightly more precise SW end-member value, and is our best estimate for the SW N isotopic composition. This result is not very sensitive, within our range of uncertainty, to the choice of the $(^{20}Ne/^{14}N)_{norm}$

ratio. For instance, $(^{20}Ne/^{14}N)_{SW}$ of 0.9 and 1.3 would yield $\delta^{15}N$ values of -302±143 ‰, and -441±210 ‰, respectively.